Electronic Supplementary Material (ESI) for Polymer Chemistry.

SUPPORTING INFORMATION

Towards universal use of DOSY as a molar mass characterization tool: Temperature dependence investigations and a software tool to process diffusion coefficients

Igor W. F. Silva,[a] Alasdair McKay,[b] Anna Sokolova[c] and Tanja Junkers[,a]*

[a] Polymer Reaction Design group, School of Chemistry, Monash University, Clayton VIC 3800, Australia;

[b] School of Chemistry, Monash University, Clayton VIC 3800, Australia;

[c] ACNS, ANSTO, Lucas Heights, NSW 2234, Australia

Contents

1. Materials 3

2. Diffusion-ordered NMR spectroscopy (DOSY-NMR) procedure 4

3. Temperature dependence of viscosity 12

4. Small Angle Neutron Scattering (SANS) 14

4.1 Equations definition 14

4.2 SANS data collection procedure and analysis 16

References 22

1. Materials

Polystyrene (PS) standards, obtained from PSS, were used to gather calibration curves in different temperatures. The molar mass range studied was 1200 to 280000 g·mol^{-1}, Table S1 presents all materials and their M_n, M_w, M_p and $Đ$. The samples were prepared in a concentration of 2 mg·mL^{-1} on toluene-d_8.

Table S1: Polystyrene standard in a molar mass range of 1200 to 280000 g·mol^{-1}.

Sample	M_n (g·mol^{-1})	M_w (g·mol^{-1})	M_p (g·mol^{-1})	$Đ$
PS1200	1120	1220	1306	1.09
PS3200	3350	3510	3500	1.05
PS9k	8420	8670	8680	1.03
PS18k	16900	17300	17600	1.03
PS33k	32700	34000	34800	1.04
PS62k	59300	62500	66000	1.05
PS120k	120000	125000	130000	1.04
PS280k	282000	294000	304000	1.04

2. Diffusion-ordered NMR spectroscopy (DOSY-NMR) procedure

The experiments were run in Bruker Neo nanobay NMR spectrometer with a 5 nm broadband BB-H/D probe operating at 400.14 MHz for ^{1}H with a ~50 G·cm^{-1} z-gradient and a BCUII cooling unit. Samples were made up at 0.5 mL and placed in 5 mm NMR tubes. A reduced volume was used for 3 mm NMR tubes. Measurements were conducted in 10 K increments in the range 273-343 K. Sample were kept stationary (not rotating) throughout the measurement unless otherwise stated. The gas flow was set to 550 L·h^{-1} to minimise convection artefacts. Samples were maintained at the desired temperature inside the magnet for at least 20 min for the sample to reach thermal equilibrium before any measurements were conducted. Measured temperature values from the thermocouple in the probehead were corrected utilising the temperature-dependent chemical shifts, of the OH group in 99.8% perdeuterated methanol.[1]

The bipolar pulse longitudinal eddy current delay (ledbgp2s) pulse program or the double-stimulated-echo (dstebpgp3s) pulse program were used,[2] with a smoothed square shaped (SMSQ) pulse.[3] Experiments were performed as pseudo-2D with a linear ramping of the gradient from 2 to 98% of maximum intensity in 32 steps. For each step, 8 transients were acquired following 8 dummy transients. The diffusion time, Δ (d20), was 100 ms, unless otherwise stated, the spoil gradient (p19) was set to 600 µs, the recycle delay (d1) was 3 s and the eddy current delay (d21) was 5 ms. The gradient pulse length, the $\delta/2$ (p30), was optimized on a per-sample basis, see Table S2.[i]

The data were processed using Topspin 4.1.4 and the peak areas, I, were used to fit the Stejskal-Tanner formula, Eq. (1), as single-component fits, to determine the diffusion coefficient, D, using Dynamics Center 2.8.3.

$$\frac{I}{I(0)} = e^{-D\gamma^2\delta^2\sigma^2 g^2\Delta'} \qquad (Eq.\ 1)$$

As discussed in the main text, convection is caused by temperature gradients within the sample, thus leading to the overestimation of diffusion coefficients.[4] Methods have been proposed to minimise these effects, such as collecting data at ambient temperature without temperature control to remove pulsing from the temperature control unit that can induce convection.[5] Conducting the experiment with optimised flow rate of the VT gas, rotating the sample, utilising sapphire NMR tubes, utilising shaped or Shigemi tubes rather than regular

[i] *Caution: care was taken such that the p30 setting did not exceed the manufacturer's recommendations in terms of the overall length of all gradients applied during a repetition period, as this may damage the NMR probe. This is particularly relevant for the dstebpgp3s pulse program. Please seek further guidance from your NMR specialist and instrument manufacturer, before undertaking these experiments.*

NMR tubes, decreasing the sample size by employing smaller inner diameter NMR tubes, inserting a small capillary contain D_2O to provide a physical barrier to convection flows, or using triaxial field gradients.[6–11] Alternatively, pulse sequences that are designed to compensate for the effects of flow on the signals measured can be employed. These sequences are typically designed to refocus the effects of a constant velocity of flow along a field gradient direction, usually by splitting the diffusion weighting sequence element into two symmetrical halves generating equal and opposite flow effects, the so-called double-stimulated-echo experiment.

The data discussed in the main text about the ledbpgp2s acquisition can be check in the following Figures. Figure S1 shows the viscosity-corrected calibration data of the ledbpgp2s pulse sequence of polystyrene standards at several temperatures. Figure S2 presents the 3D calibration of viscosity-corrected diffusion coefficients as a function of temperature and molar mass of polystyrene standards, same data acquired on Figure S1.

The methods applied to decrease convection effects in DOSY experiments: acquiring diffusion data whilst rotating the sample and using 3 mm NMR tubes (instead of 5 mm usual tubes). Figure S3 compares the molar mass estimation curves acquired by ledbpgp2s, no rotation of the sample (S3a), ledbpgp2s, rotating the sample (S3b), ledbpgp2s, no rotation, using 3 mm NMR tubes (S3c) and dstebpgp3s, no rotation, using 5 mm NMR tubes (S3d). Figure S4 compares the viscosity-corrected calibration of diffusion coefficients determined via DOSY using ledbpgp2s and dstebpgp3s pulse programs for polystyrene standards at 293 K (20 °C).

Figure S5 compares the logarithmic DOSY signal intensities of the polymer signals against the square of gradient strength acquired by ledbpgp2s, no rotation of the sample (S5a), ledbpgp2s, rotating the sample (S5b), ledbpgp2s using 3 mm NMR tubes (S5c) and dstebpgp3s no rotation and using 5 mm NMR tubes (S5d) in temperatures, where convection artefacts are present in the diffusion data.

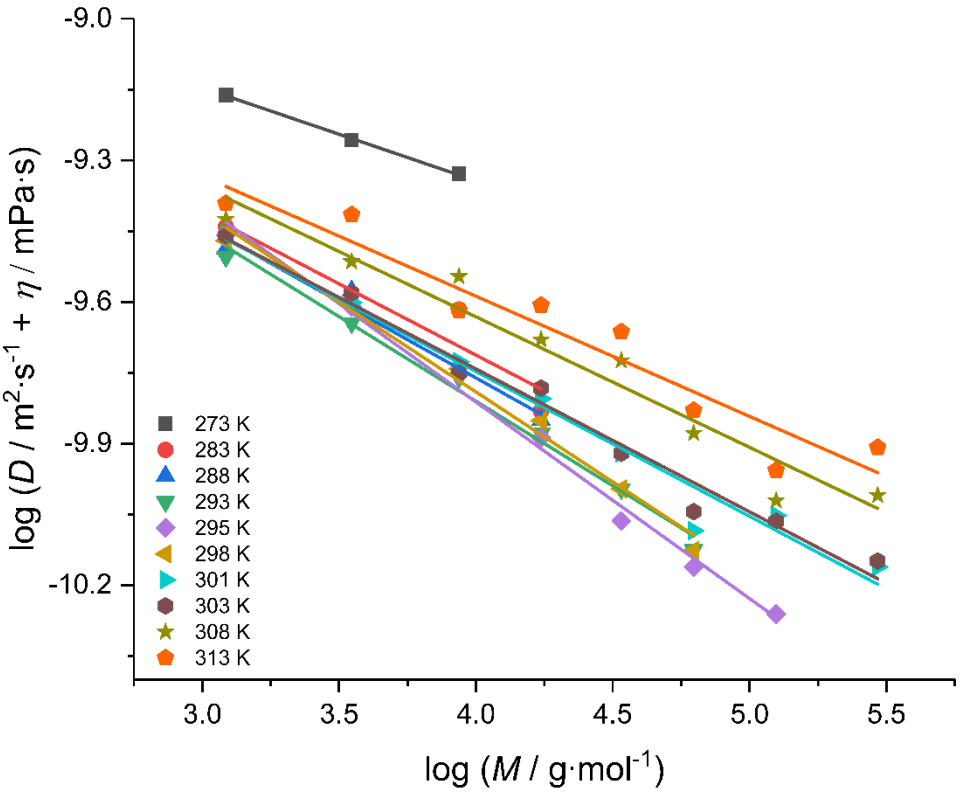

Figure S1. Viscosity-corrected calibration data of polystyrene standards at several temperatures measured using ledbpgp2s pulse sequence.

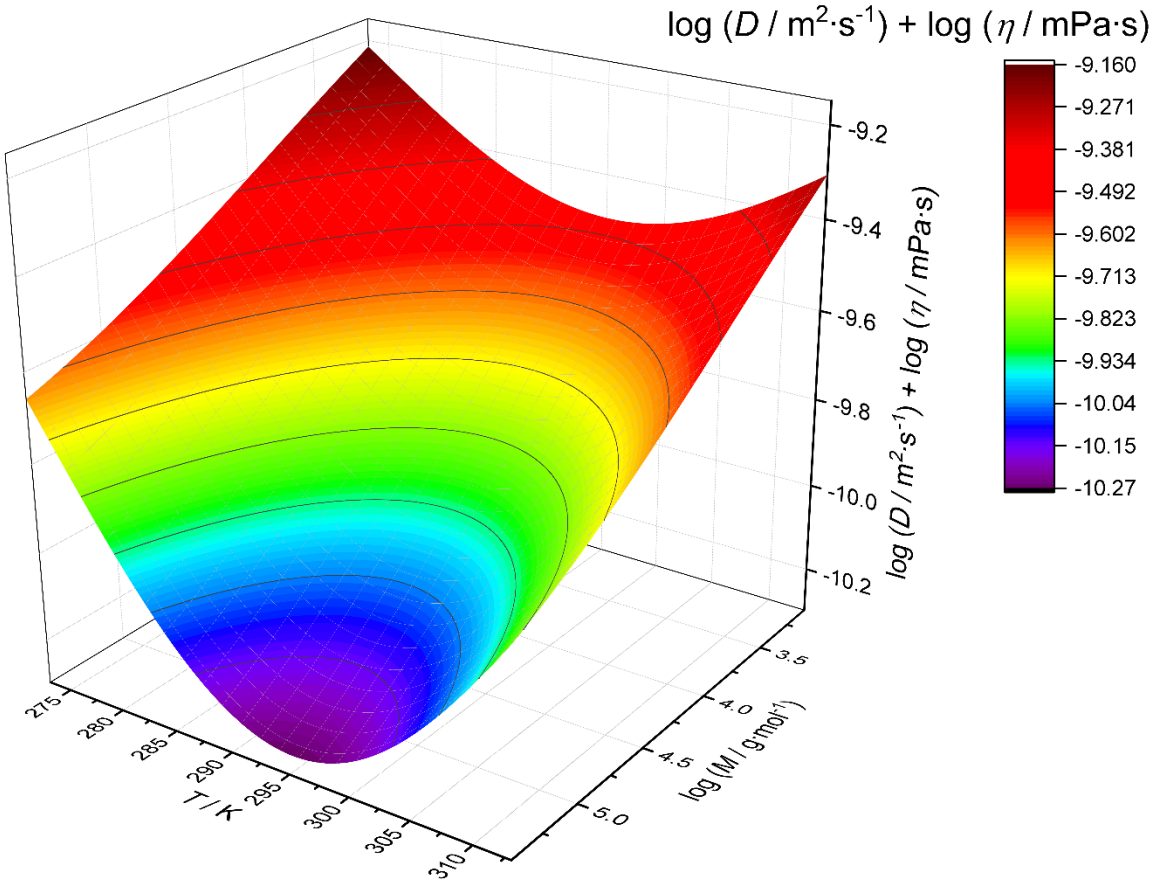

Figure S2. 3D calibration fit of viscosity-corrected diffusion coefficients (obtained using ledbpgp2s) as a function of temperature and molar mass of polystyrene standards.

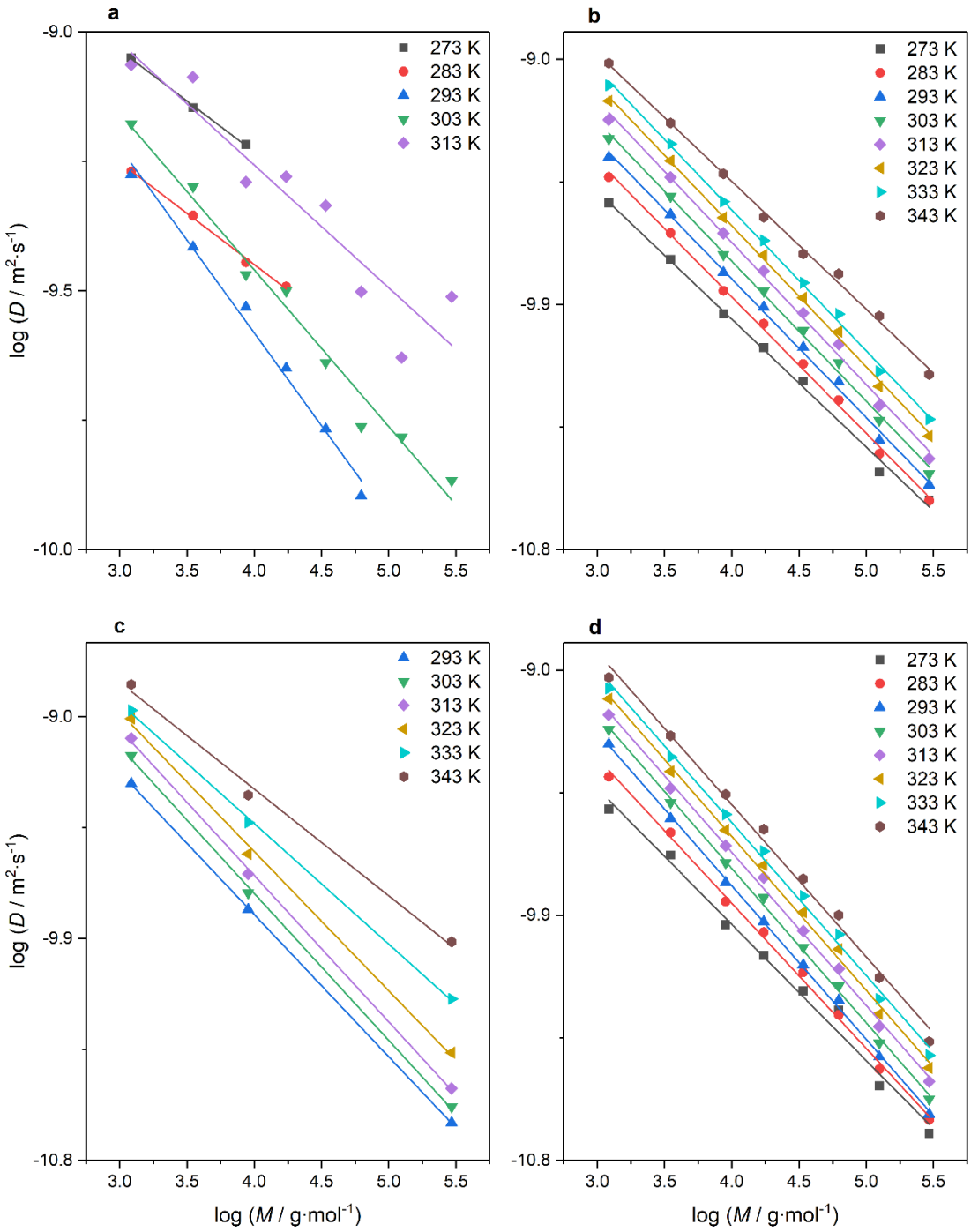

Figure S3. Calibration curves between molar mass and diffusion coefficient acquired by the using the following conditions: ledbpgp2s, no rotation of the sample (a), ledbpgp2s, rotating the sample (b), ledbpgp2s, no rotation, 3 mm NMR tubes (c) and dstebpgp3s, no rotation, 5 mm NMR tubes (d). Data was acquired in temperatures between 273 and 343 K (0 and 70 °C).

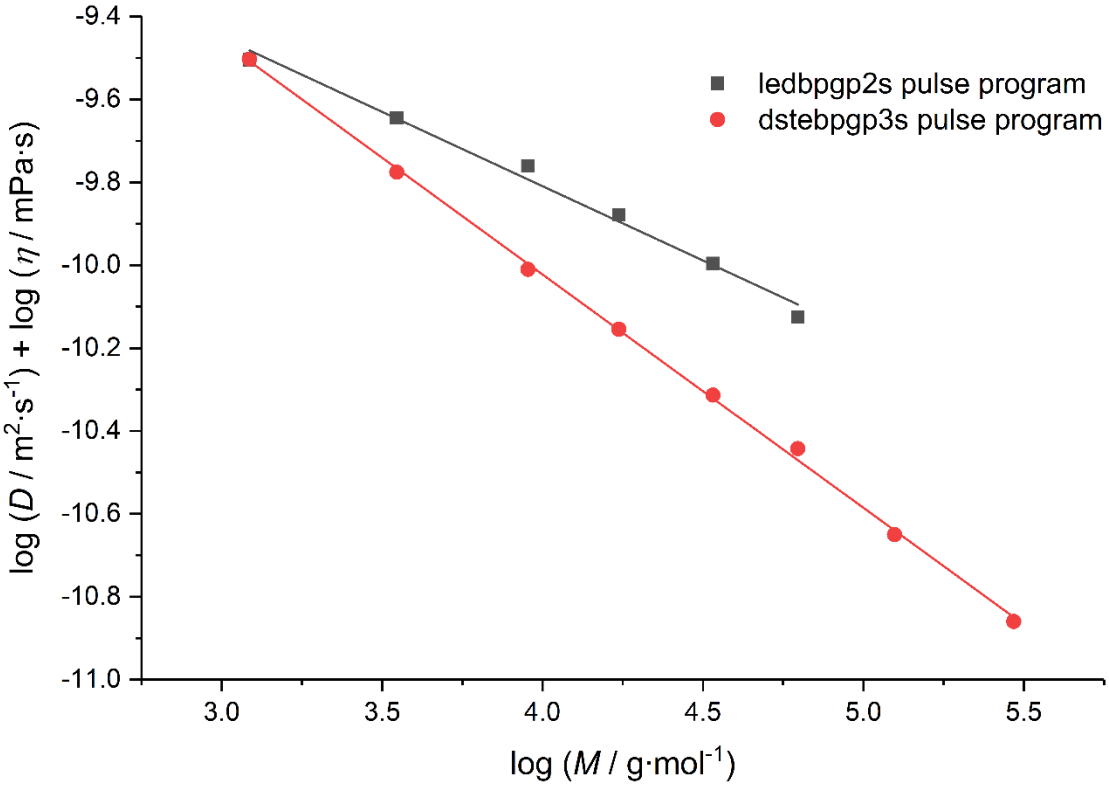

Figure S4. Viscosity-corrected calibration of diffusion coefficients determined via DOSY (acquired by ledbpgp2s (grey) and dstebpgp3s (red) pulse programs) for polystyrene standards at 293 K (20 °C).

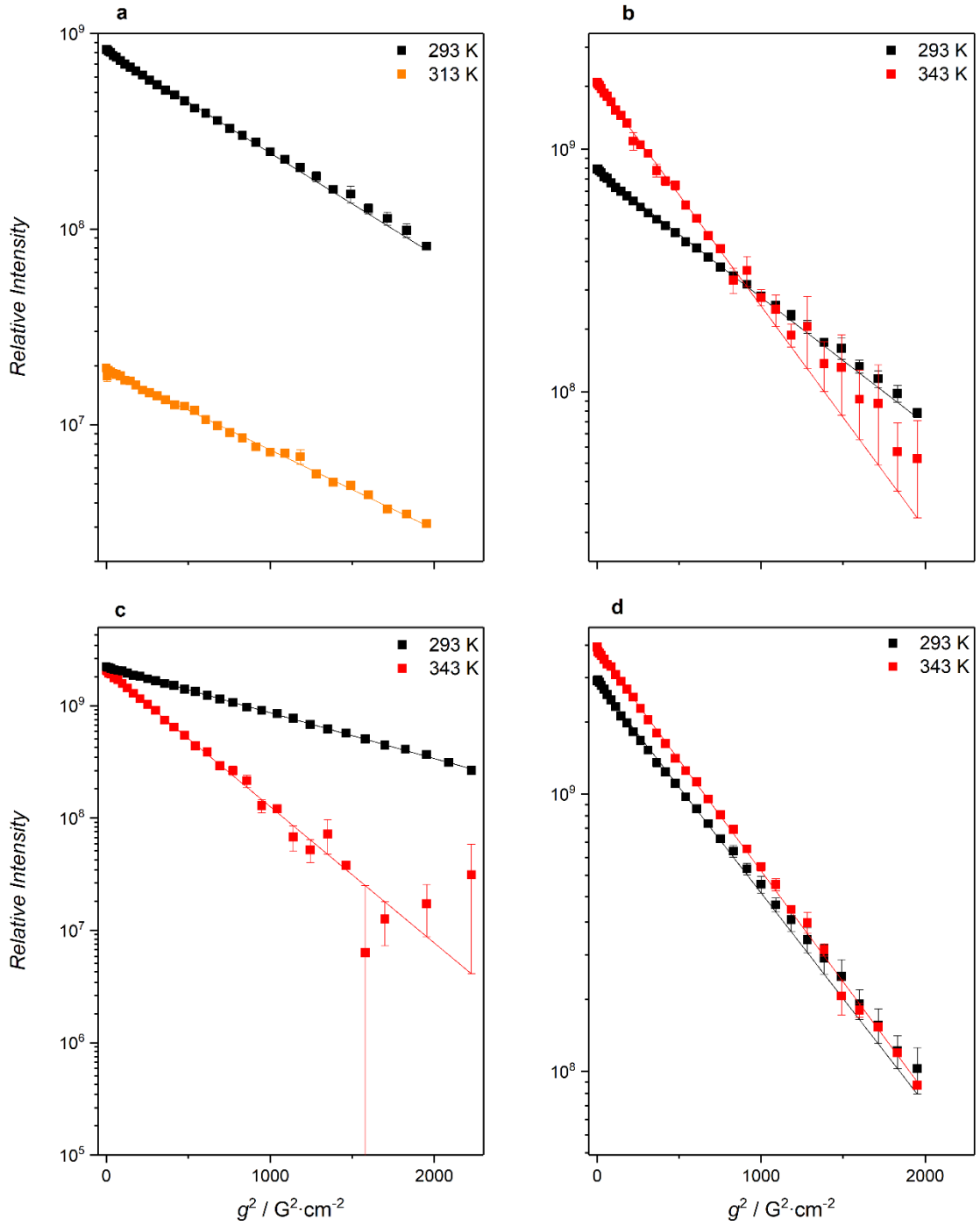

Figure S5. Logarithmic DOSY signal intensities of the polymer signals against the square of gradient strength acquired by ledbpgp2s, no rotation of the sample (a), ledbpgp2s rotating the sample (b), ledbpgp2s using 3 mm NMR tubes (c) and dstebpgp3s no rotation and using 5 mm NMR tubes (d) in temperatures, which demonstrate convection artefacts.

Table S2. Gradient pulse lengths (δ/2; p30, μs) for standard PS samples in different temperatures (**ledbpgp2s**).

Samples	273 K	283 K	288 K	293 K	295 K	298 K	301 K	303 K	308 K	313 K
PS1200	800	800	800	800	800	800	1000	1000	800	800
PS3200	800	1000	1000	1000	1000	1000	1000	1000	800	800
PS9k	1000	1000	1200	1200	1200	1000	1000	1000	800	800
PS18k	1000	1000	1200	1400	1400	1200	1200	1200	1000	1000
PS33k	-	1200	1400	1400	1400	1400	1200	1200	1000	1000
PS62k	-	-	-	1600	1600	1400	1200	1200	1000	1000
PS120k	-	-	-	-	1600	1600	1600	1600	1200	1200
PS280k	-	-	-	-	-	1600	1600	1600	1200	1200

Table S3. Gradient pulse lengths (δ/2; p30, μs) for standard PS samples in different temperatures (**dstebpgp3s**).

Samples	273 K	283 K	293 K	303 K	313 K	323 K	333 K	343 K
PS1200	900	900	900	900	900	800	800	800
PS3200	1000	1000	1000	1000	1000	1000	1000	1000
PS9k	1600	1600	2000	1600	1600	1600	1600	1400
PS18k	1600	1600	2000	1800	1800	1800	1600	1600
PS33k	1600	1600	2000	2000	2000	1800	1600	1600
PS62k	1600	2000	2000	2000	2000	1800	1800	1600
PS120k	2000	2200	2200	2200	2200	2000	2000	2000
PS280k	2200	2200	2200	2200	2200	2200	2200	2200

3. Temperature dependence of viscosity

Figure S6 shows temperature dependence data of viscosity[12] (solid squares) used to build a third-order polynomial fitting function of $\eta(T)$ (r^2 = 0.99997). The values used in this work (open squares) were taken from this fitting function. The exact values of η used for each temperature can be checked in Table S4 (on the right).

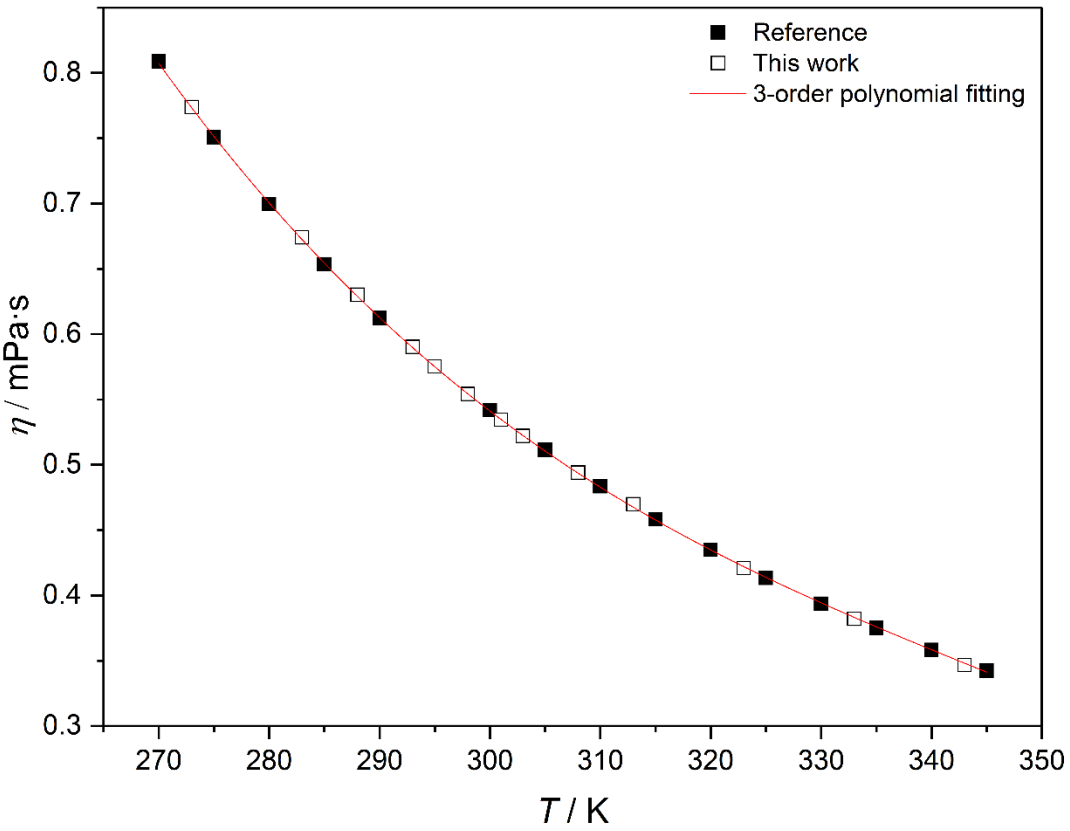

Figure S6. Viscosity (η) of toluene in the function of temperature (T), where solid squares are data from the reference[12], open squares are the temperatures used in DOSY-NMR, and the red line is 3-order polynomial fitting of the reference data.

Table S4. Values of viscosity (η) and temperature (T) from the reference[12] and used in this work.

Reference[12]		Values for this work	
T (K)	η (mPa·s)	T (K)	η (mPa·s)
270	0.8087	273	0.7738
275	0.7508	283	0.6740
280	0.6994	288	0.6301
285	0.6535	293	0.5901
290	0.6124	295	0.5752
295	0.5753	298	0.5541
300	0.5418	301	0.5344
305	0.5113	303	0.5220
310	0.4835	308	0.4939
315	0.4581	313	0.4698
320	0.4348	323	0.4207
325	0.4133	333	0.3819
330	0.3935	343	0.3467
335	0.3751	-	-
340	0.3581	-	-
345	0.3423	-	-

4. Small Angle Neutron Scattering (SANS)

4.1 Equations definition

Scheme S1 shows neutrons, with a wavelength λ, interacting with the sample and scattering from it. The incident neutrons on the sample have a momentum $\overrightarrow{k_i}$ and the scattered neutrons by the sample have a momentum $\overrightarrow{k_f}$. The angle between the two vectors is the scattering angle, 2θ.[13]

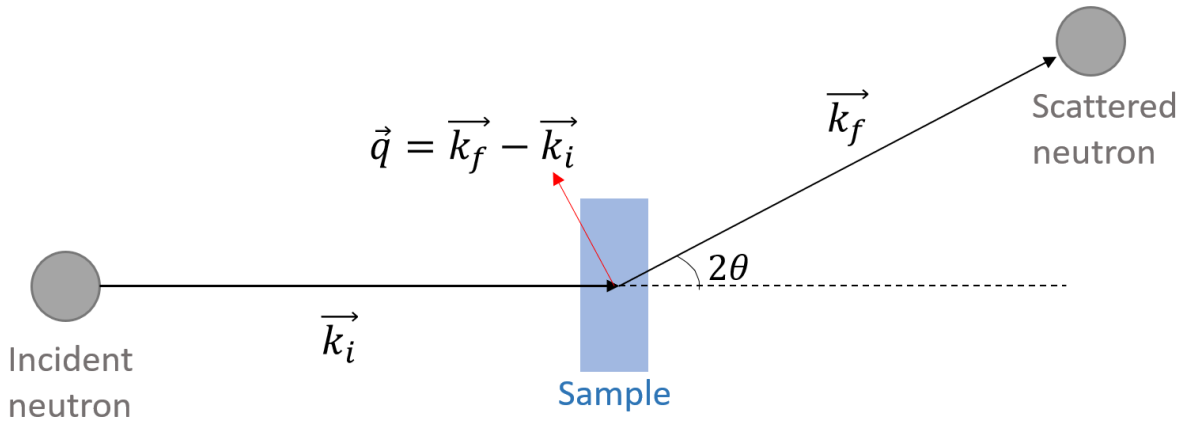

Scheme S1. Definition of the momentum transfer ($\vec{q}$) in Small-Angle Neutron Scattering measurements.

Considering only elastic scattering, it is possible to assume:

(*Eq. 2*) $$\|\overrightarrow{k_i}\| = \|\overrightarrow{k_f}\| = \frac{2\pi}{\lambda}$$

SANS data are acquired as a function of the momentum transfer:

(*Eq. 3*) $$\vec{q} = \overrightarrow{k_f} - \overrightarrow{k_i}$$

,which the magnitude of the momentum transfer is defined by:

(*Eq. 4*) $$\|\vec{q}\| = q = \frac{4\pi}{\lambda}\sin\left(\frac{2\theta}{2}\right)$$

The scattering intensity of the polymer coils was modelled ('*poly_gauss_coil*' from SASView) *via*[14,15]:

(*Eq. 5*) $$I(q) = \phi_p \cdot V_p \cdot \Delta SLD^2 \cdot P(q) + I_{bkg}$$

Where $I_{coil}(q)$ is the scattering intensity of a polymer coil with excluded volume effects, I_{bkg} the incoherent background, and ϕ_p and V_p the volume fraction and molecular volume of the polymer, respectively. V_p can be defined as $V_p = \frac{M}{N_A \delta}$, where M is the molar mass

of the polymer, N_A is the Avogadro's Number, and δ is the bulk density of the polymer. The polymer coil form factor[16] $P(q)$ is described as:

(*Eq. 6*) $$P(q) = 2\left[\frac{(1+UZ)^{-1/U}+Z-1}{(U+1)Z^2}\right]$$

where

(*Eq. 7*) $$Z = \frac{(qR_g)^2}{1+2U}$$

(*Eq. 8*) $$U = Đ - 1$$

The relation between the scattering intensity and the characteristic of a particle is also given by the Fourier transformation[17]:

(*Eq. 9*) $$I(q) = 4\pi \int_0^\infty p(r)\frac{\sin(qr)}{qr}dr$$

Where the distribution of interatomic distances, $p(r)$, is calculated as $p(r) = \gamma(r) \cdot r^2$ where $\gamma(r)$ is a spherically averaged autocorrelation function of the excess scattering density. The distribution becomes zero at $r = 0$ and $r = D_{max}$.

(*Eq. 10*) $$p(r) = \frac{r^2}{2\pi^2}\int_0^\infty q^2 I(q)\frac{\sin qr}{qr}\mathrm{d}q$$

R_g has been calculated using Primus software using the following relation:

(*Eq. 11*) $$R_g^2 = \frac{\int_V p(r)r^2dr}{\int_V p(r)dr}$$

4.2 SANS data collection procedure and analysis

The SANS experiments were performed in the Bilby SANS instrument at the Australian Centre for Neutron Scattering (ACNS), ANSTO. The temperatures used in the experiments were of 279, 283, 292, 295, 298 and 308 K. The polymer samples used for this experiment were the PS9k, PS33k, PS62k and PS120k (see Table S1). The samples were carried out on toluene-d_8 at the concentration of 2 mg·mL^{-1}. The measurement time for the polymers solutions was 3600 s, and that for the toluene of the matching temperatures was 1500 s. Instrument has been set-up in a time-of-flight mode. Data has been reduced on wavelength interval from 4 Å to 12 Å covering q-range from 0.003 Å^{-1} to -0.52 Å^{-1}. Rear detector has been placed 18 m away from the samples, vertical curtains were 1 m away, and vertical ones are 2 m, with 0.3 m, 0.35 m, 0.075 m and 0.15 m separation from the beam for the left, right, top and vertical ones, correspondingly. Backgrounds has been considered and data placed on the absolute scale using standard Bilby procedures, implemented in Mantid[18,19] software. Scattering from the solvent has been carefully subtracted.

The software used to process the data were the SASview 5.0.6 (https://www.sasview.org)[20]. The data were fitted using '*poly_gauss_coil*' model. The dispersity was adjusted to the values of Table S1, and the scale was kept constant for each given polymer. To assess the overall structural properties, Primus[21] software from ATSAS suit has been used to calculate $p(r)$ functions and R_g values based on $p(r)$, and also create Kratky plots to estimate level of folding/unfolding for each polymer.

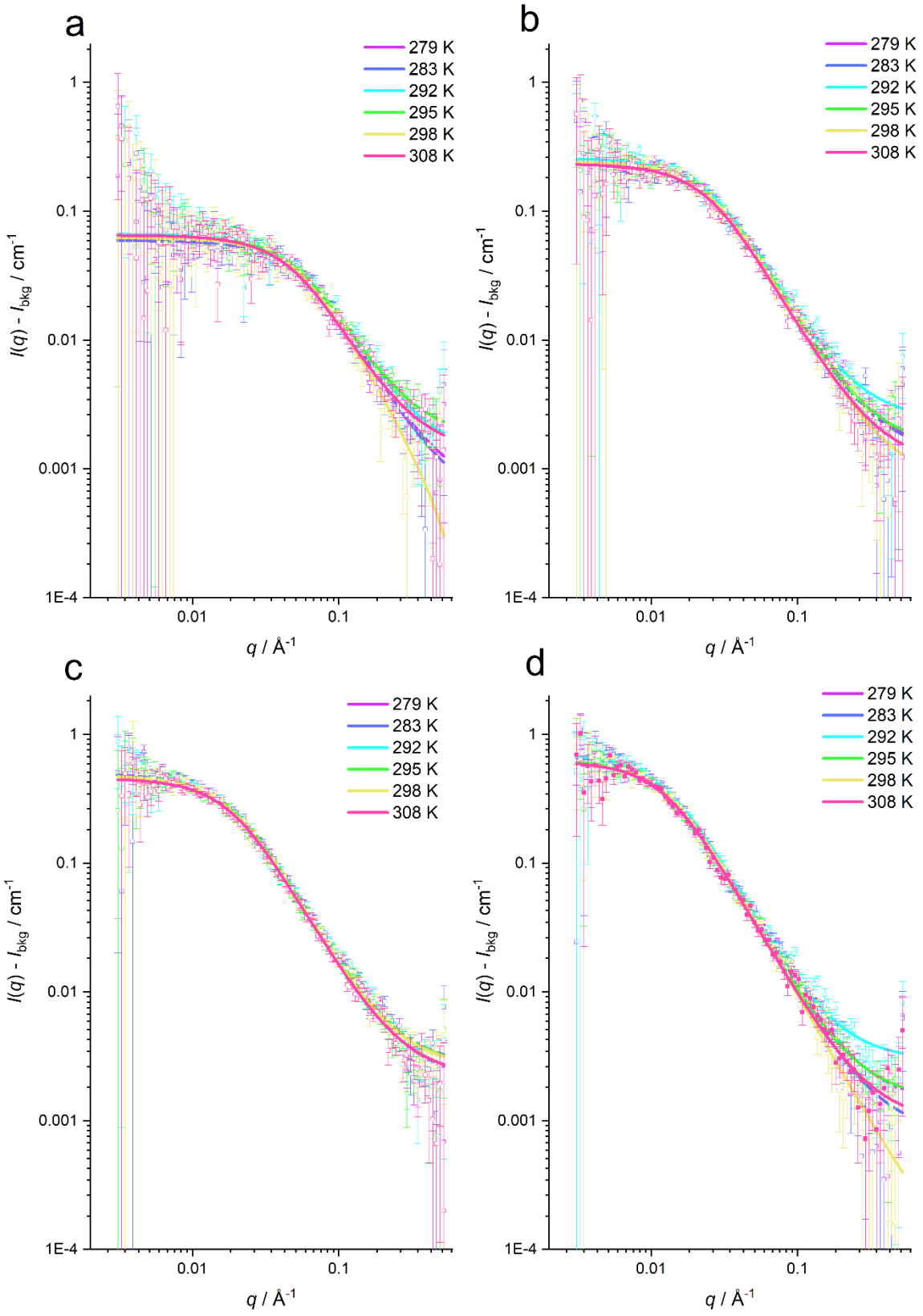

Figure S7. SANS data of standard polystyrene (average molar mass of 9 (a), 33 (b), 62 (c), and 120 (d) kg·mol^{-1}) in different temperatures. The squares represent the experimental data and the lines represent the Gaussian polymer coil fits for each temperature.

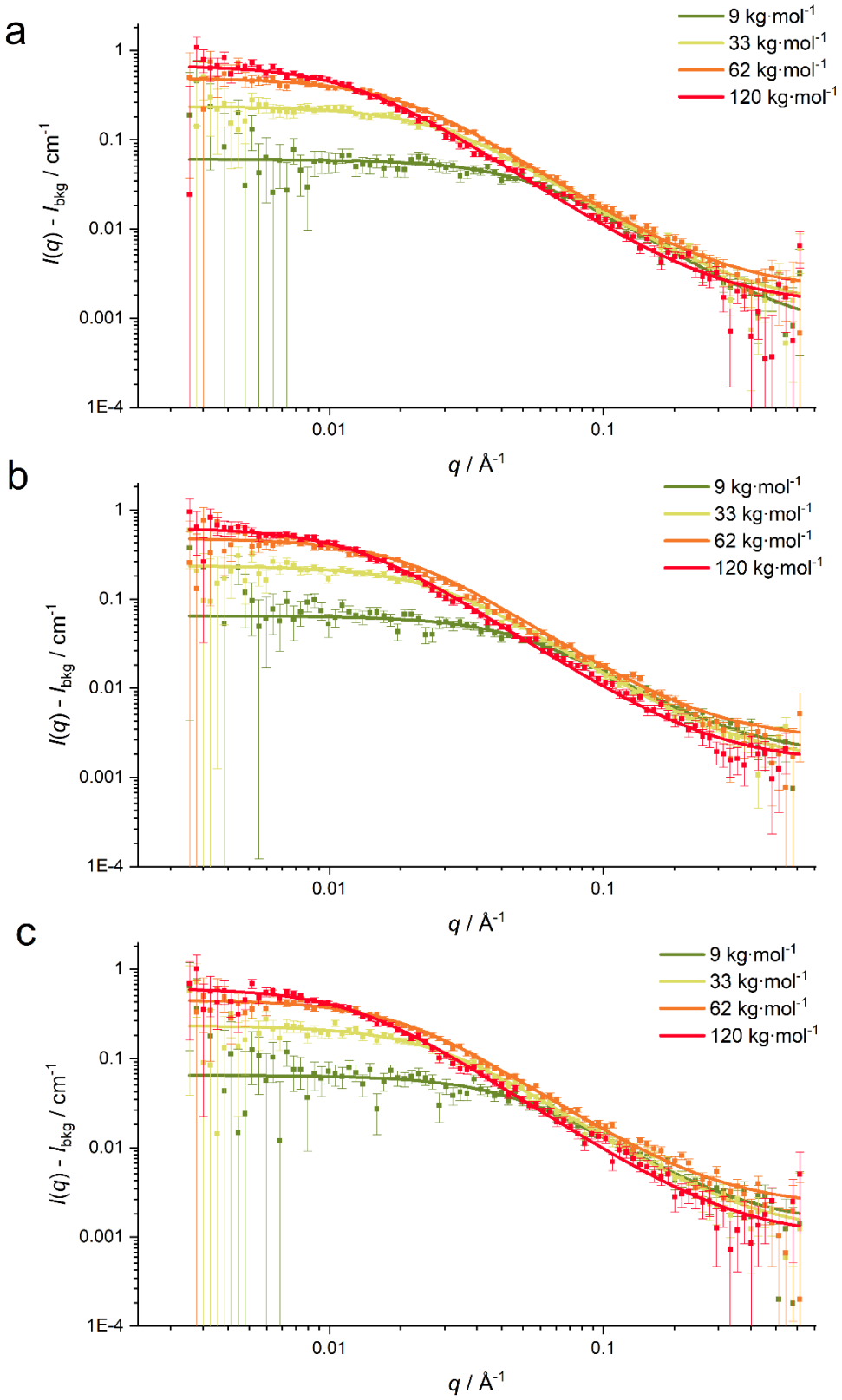

Figure S8. SANS data of standard polystyrene (average molar mass of 9, 33, 62, and 120 kg·mol^{-1}) at the temperatures of 279 (a), 295 (b), and 308 (c) K. The squares represent the experimental data and the lines represent the Gaussian polymer coil fits for each temperature.

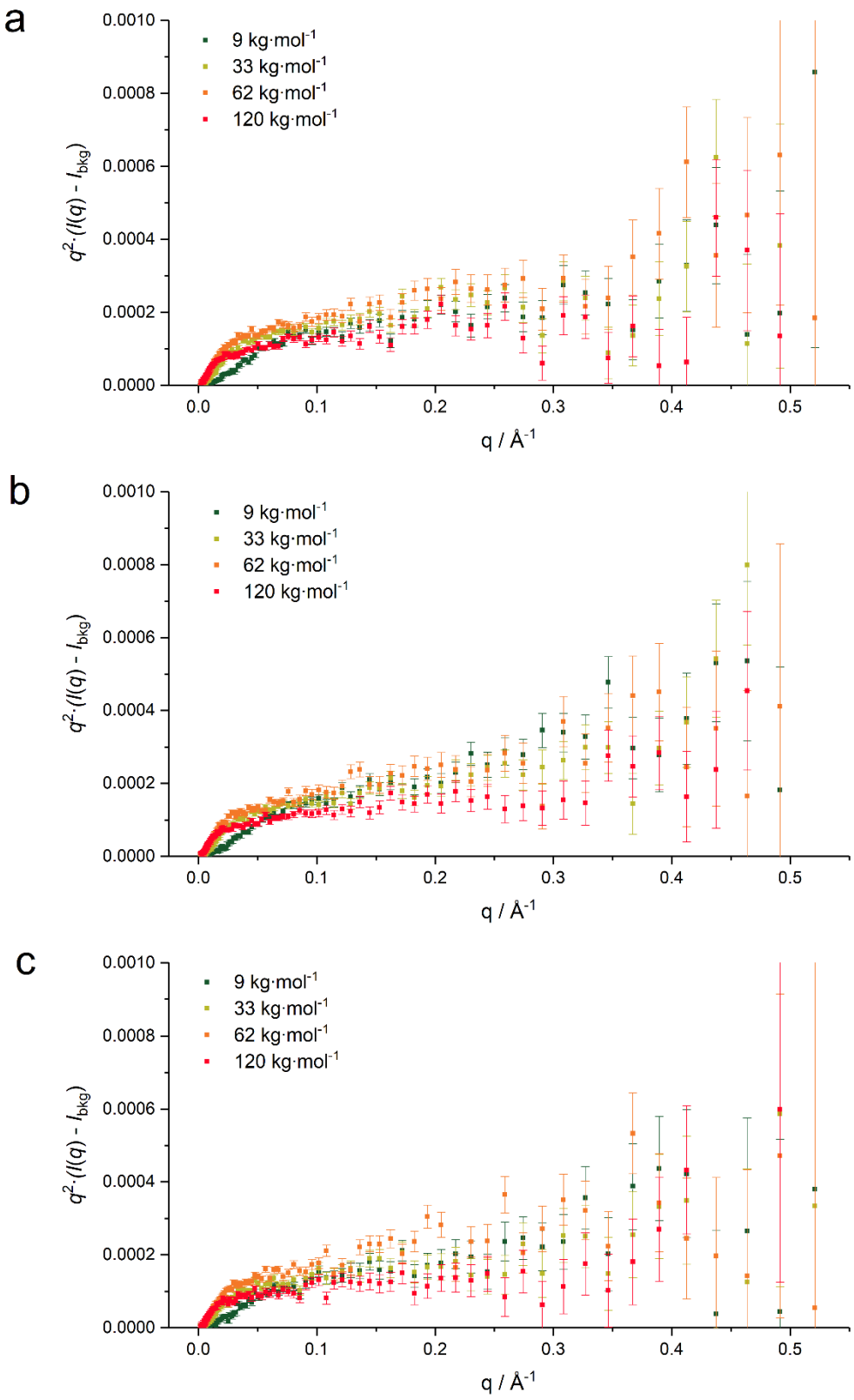

Figure S9. Kratky plots of SANS data of standard polystyrene (average molar mass of 9, 33, 62, and 120 kg·mol^{-1}) at the temperatures of 279 (a), 295 (b), and 308 (c) K. The squares represent the experimental data and the lines represent the Gaussian polymer coil fits for each temperature.

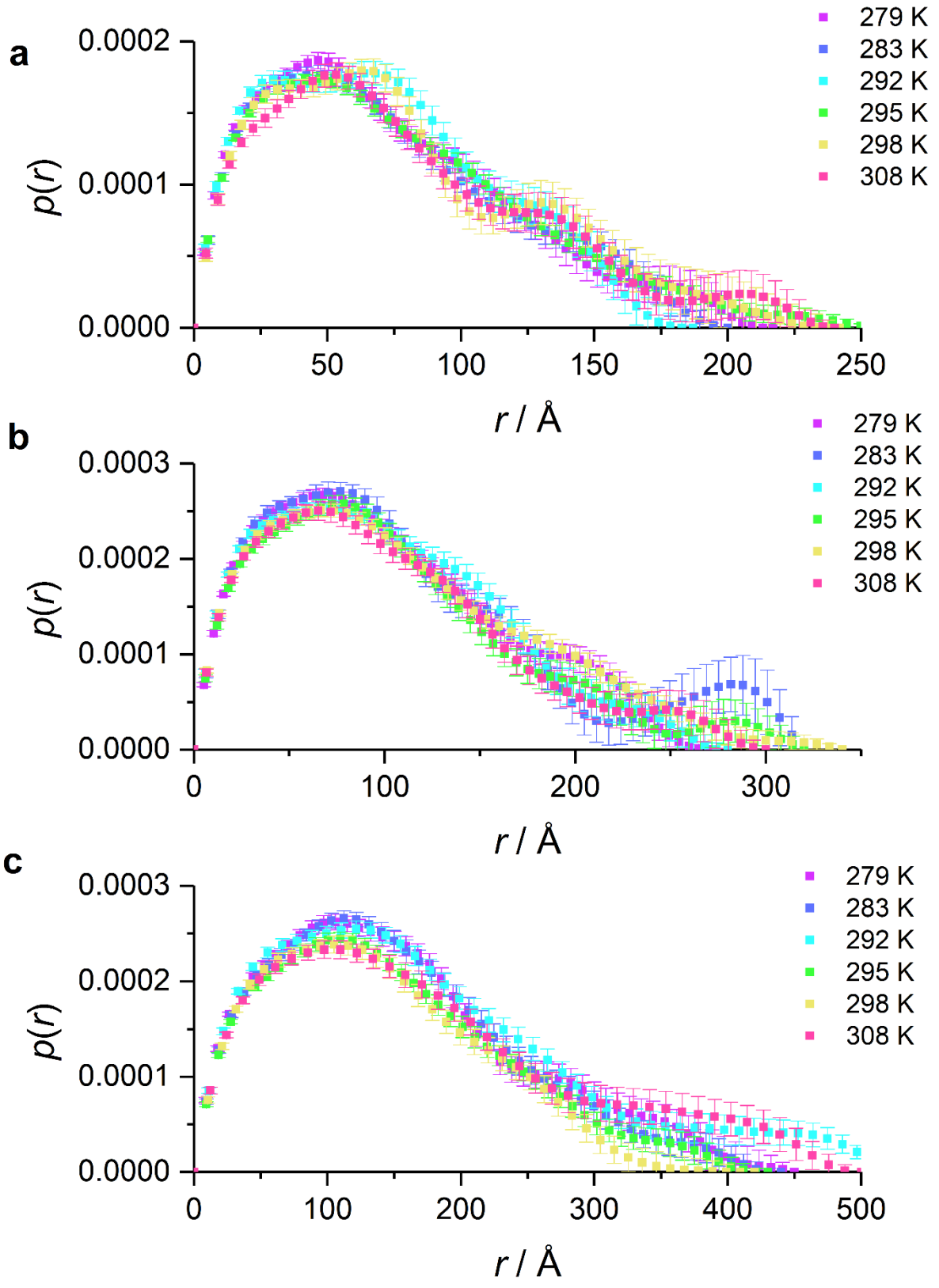

Figure S10. p(r) curves of SANS data of standard polystyrene (average molar mass of 33 (a), 62 (b), and 120 (c) kg·mol^{-1}) in different temperatures.

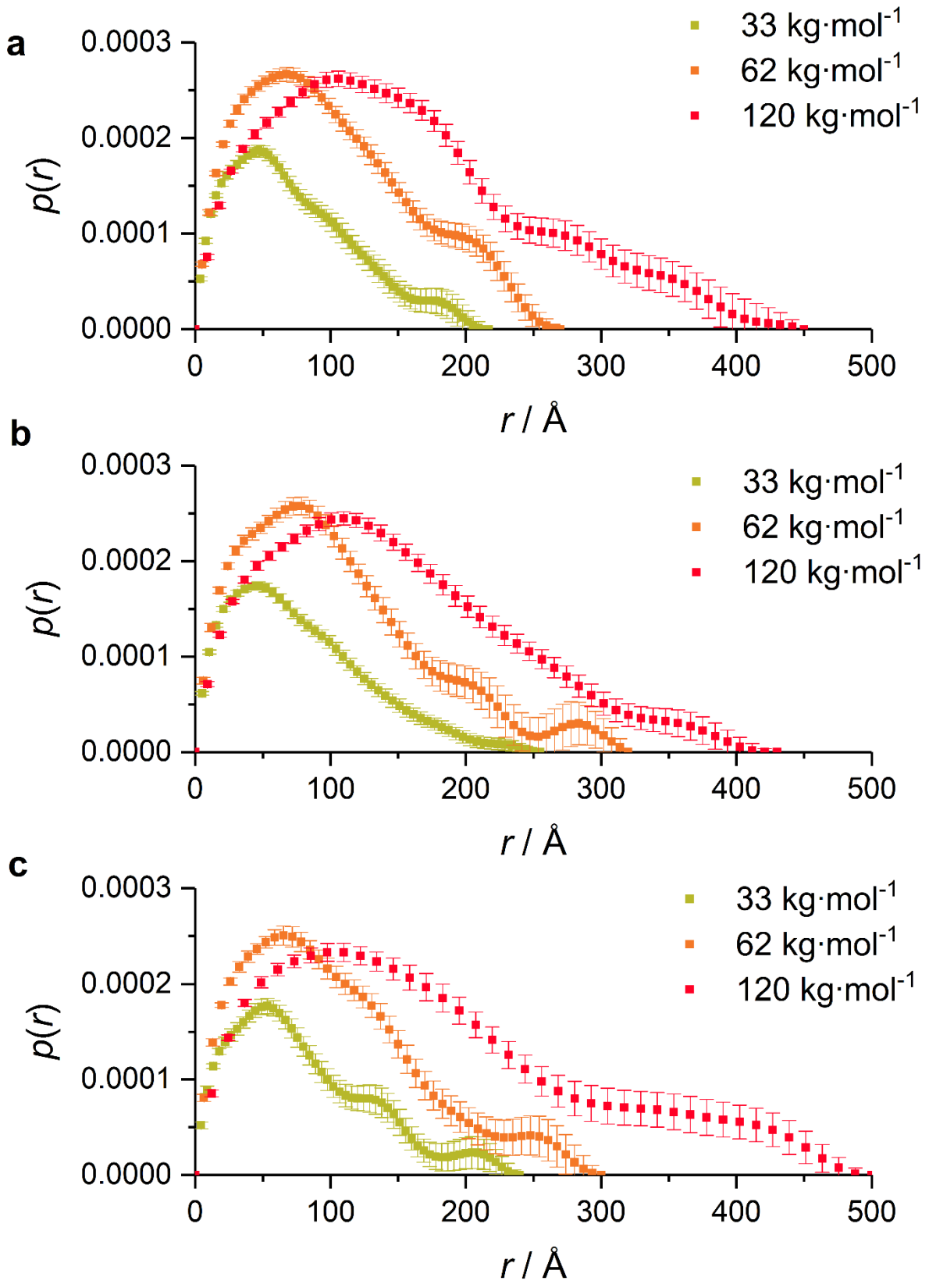

Figure S11. p(r) curves of SANS data of standard polystyrene (average molar mass of 33, 62, and 120 kg·mol^{-1}) at the temperatures of 279 (a), 295 (b), and 308 (c) K.

References

1 A. L. Van Geet, *Anal. Chem.*, 1968, **40**, 2227–2229.
2 S. J. Gibbs and C. S. Johnson, *Journal of Magnetic Resonance (1969)*, 1991, **93**, 395–402.
3, DOI:10.1002/cmr.a.21223.
4 G. H. Sørland and D. Aksnes, *Magnetic Resonance in Chemistry*, 2002, **40**, S139–S146.
5 P. Groves, *Polym. Chem.*, 2017, **8**, 6700–6708.
6 I. Swan, M. Reid, P. W. A. Howe, M. A. Connell, M. Nilsson, M. A. Moore and G. A. Morris, *Journal of Magnetic Resonance*, 2015, **252**, 120–129.
7 P. Kiraly, I. Swan, M. Nilsson and G. A. Morris, *Journal of Magnetic Resonance*, 2016, **270**, 24–30.
8 C. R. Pope, M. Kar, D. R. MacFarlane, M. Armand, M. Forsyth and L. A. O'Dell, *ChemPhysChem*, 2016, **17**, 3187–3195.
9 K. Hayamizu and W. S. Price, *Journal of Magnetic Resonance*, 2004, **167**, 328–333.
10 N. Esturau, F. Sánchez-Ferrando, J. A. Gavin, C. Roumestand, M.-A. Delsuc and T. Parella, *Journal of Magnetic Resonance*, 2001, **153**, 48–55.
11 J. Lounila, K. Oikarinen, P. Ingman and J. Jokisaari, *Journal of Magnetic Resonance, Series A*, 1996, **118**, 50–54.
12 F. J. V. Santos, C. A. Nieto De Castro, J. H. Dymond, N. K. Dalaouti, M. J. Assael and A. Nagashima, *Journal of Physical and Chemical Reference Data*, 2006, **35**, 1–8.
13 W. T. Heller, *Biomolecules*, 2022, **12**, 1591.
14 P. Debye and A. M. Bueche, *Journal of Applied Physics*, 2004, **20**, 518–525.
15 A. Guinier, G. Fournet, C. B. Walker and G. H. Vineyard, *Physics Today*, 1956, **9**, 38–39.
16 B. Hammouda, in *Polymer Characteristics*, Springer, Berlin, Heidelberg, 1993, pp. 87–133.
17 O. Glatter, *J Appl Cryst*, 1977, **10**, 415–421.
18 Mantid Project, Mantid: Manipulation and Analysis Toolkit for Instrument Data 2013.
19 O. Arnold, J. C. Bilheux, J. M. Borreguero, A. Buts, S. I. Campbell, L. Chapon, M. Doucet, N. Draper, R. Ferraz Leal, M. A. Gigg, V. E. Lynch, A. Markvardsen, D. J. Mikkelson, R. L. Mikkelson, R. Miller, K. Palmen, P. Parker, G. Passos, T. G. Perring, P. F. Peterson, S. Ren, M. A. Reuter, A. T. Savici, J. W. Taylor, R. J. Taylor, R. Tolchenov, W. Zhou and J. Zikovsky, *Nuclear Instruments and Methods in Physics Research Section A: Accelerators, Spectrometers, Detectors and Associated Equipment*, 2014, **764**, 156–166.
20 NSF project, SasView.
21 K. Manalastas-Cantos, P. V. Konarev, N. R. Hajizadeh, A. G. Kikhney, M. V. Petoukhov, D. S. Molodenskiy, A. Panjkovich, H. D. T. Mertens, A. Gruzinov, C. Borges, C. M. Jeffries, D. I. Svergun and D. Franke, *J Appl Cryst*, 2021, **54**, 343–355.